Visual Observations of a Turbulent Diffusion Flame

M. G. MUNGAL AND J. M. O'NEIL*

Mechanical Engineering Department, Stanford University, Stanford, CA 94305

High-speed visual observations of a turbulent, momentum-driven, acetylene diffusion flame are presented. It is found that the flame tip burnout can be interpreted as a consequence of the large-scale organized motion in the flow—at times the tip burnout is axisymmetric in nature while at other times it appears more helical. These observations are similar to and were motivated by, the measurements by Dahm and Dimotakis on liquid "flames." The results are consistent with previous soot measurements of Magnussen on similar turbulent flames.

INTRODUCTION

There have been numerous studies of turbulent diffusion flames in the past. Some of these have dealt with detailed measurements of the temperature and velocity fields [1], effects of buoyancy [2, 3], flame length observations [4], soot emission [5–10], and effects of burner orientation [11]. A separate body of work has dealt with the near field of jet flames [12–14]. Additional works have dealt with flame liftoff [15] and flame blowout [16].

Perhaps less well known to the combustion community are earlier experiments of Weddell (see Ref. 17) in which acid–base chemical reactions were used to simulate turbulent "flames" in water. Heat release effects and consequently buoyancy effects were absent in Weddell's flames. This approach of using acid–base chemistry to study the fluid mechanics of mixing in round turbulent jets has recently been continued by Dahm and Dimotakis [18] taking advantage of a laser sheet and a fluorescent dye to observe the turbulent mixing in "cuts" or "slices" through the jet centerline. Proper choice of acid–base concentrations were used to simulate flames of any desired stoichiometric ratio.

A striking finding of Dahm and Dimotakis was that the far field of the jet flame was quite organized, as evidenced by the fact that the flame tip "burned" out in a quasiperiodic fashion at a frequency that scaled with the local jet centerline velocity and local jet width, i.e., with the local large-scale variables. This key observation was not derived from single still photos of the flow, but from a movie sequence in which the tip evolution and burnout could be observed. Figure 1a, from Ref. 18, of a downward pointing liquid "flame" at a Reynolds number of 10,000 and overall length of 150 jet diameters shows the organized tip burnout. In this figure the reader is encouraged to sight along the time axis to observe the flame tip oscillation.

Movie sequences such as these lead Dahm and Dimotakis to suggest a cartoon depicting the axisymmetric concentration field resulting from the organized motion in round turbulent jets. Figure 1b, from Ref. 18, suggests that the entrainment of the surrounding reservoir fluid occurs primarily from the upstream or backside of the dominant vortical structures that from a nested set in the downstream direction. A key feature of each structure is that the instantaneous jet fluid concentration is roughly uniform throughout (as opposed to Gaussian) with the entrained and mixed fluid distributed in such a way that the time-mean concentration field obeys the required $1/x$ decay. It is also important to note that because of the three-dimensional nature of the proposed large

Present address: General Dynamics, Fort Worth, TX.

Published by Elsevier Science Publishing Co., Inc.
655 Avenue of the Americas, New York, NY 10010

0010-2180/89/$03.50

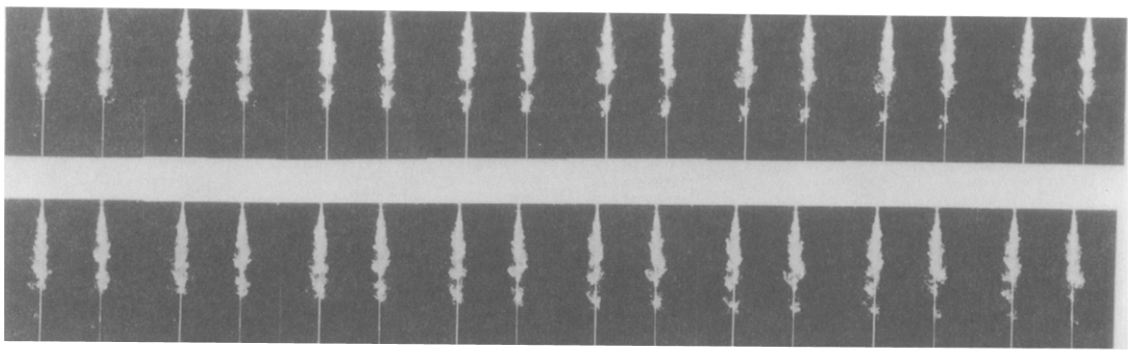

Fig. 1a. Movie sequence of round, turbulent liquid jet "flame" discharging from top to bottom. Reynolds number = 10,000. Mean flame length = $150d_0$. Framing range = 40 Hz. From Dahm & Dimotakis [18].

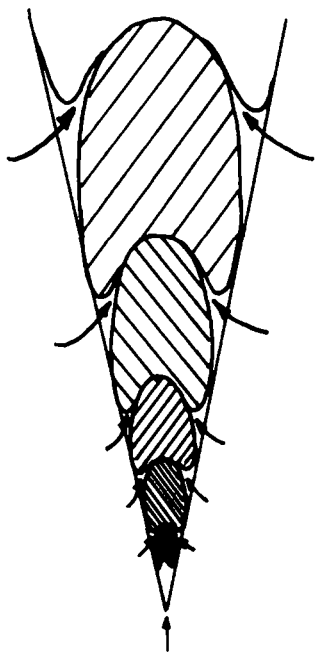

Fig. 1b. Proposed concentration field and entrainment pattern of a round turbulent jet. From Dahm and Dimotakis [18].

structure, shadowgraph pictures of the jet reveal little organized structure, as was the case for the mixing layer by Brown and Roshko [19]. Thus for the jet flow, the use of the laser sheet, fluorescent dyes, chemistry, and a movie sequence was crucial to revealing the organized structure.

Since the Dahm and Dimotakis experiments were performed in water, it is not clear what the implication is for gaseous combustion situations where heat release effects are present. Such questions were originally addressed by Broadwell [20], who proposed a jet mixing model that makes explicit use of the idea of the turbulent cascade and large-scale motion. He argues that for momentum driven jet flows of sufficiently high Reynolds number, the fluid mechanics of liquid and gaseous flows would be similar, leading to similar mixing fields. In support of this contention, a correlation was proposed by Broadwell in which the visual flame lengths of burning jets and liquid flames could be collapsed onto the same curve. Thus, it appears that there is much in common between these seemingly disparate flow situations. This correlation has been further amplified by Dahm and Dimotakis [18] (see their Fig. 1), who show that a very wide range of substances appear to collapse onto the earlier gas-liquid flame correlation.

To indicate the usefulness of this approach we note the Tyson, et al. [21], using the Broadwell jet mixing model, have been able to successfully predict the Reynolds number dependence of nitric oxide formation in turbulent jet diffusion flames, observed by Bilger and Beck [22] and Peters and Donnerhack [23]. Furthermore, Broadwell, et. al. [24] were able to propose a stabilization mechanism motivated in part by the movie sequences of liquid flames, and were able to correlate the observed blowout speeds for a wide range of common fuels reported by Kalghatgi [16]. The flame blowout model has recently been extended by Dahm and Dibble [25] to coflowing jets. Bilger

[26] has also recently provided an alternate view to mixing in turbulent jets.

Based on the comments above, an obvious question is whether the flame tip oscillations observed in liquid flames have also been observed for gaseous burning jets, under momentum-controlled conditions, for as such they would provide a clue to the far-field mixing and burning mechanisms. A search of the literature revealed little specific discussions of the flame tip dynamics. The studies cited above, with the exception of Miake-Lye and Toner [2] and the near-field studies [12–14], have tended to discuss time-averaged and fluctuating quantities without specific discussions of the structural aspects and evolution of the flame. Some discussion of fluctuations can be found in Peters and Williams [27] and Williams [28], but these are tied to the more traditional turbulence viewpoint. For these reasons, it was decided to attempt to document a turbulent momentum-driven diffusion flame with specific interest in observing the time evolution of the flame tip region in order to provide clues about the role of large-scale organized motion.

FLAME SIZING

A primary requirement of this study was to operate as close to the momentum-driven regime as possible. Becker and Yamazaki [1], in a detailed study of the effects of buoyancy upon turbulent jet flames, have proposed criteria that can be used to determine whether a given flame is influenced by buoyancy. These guidelines were followed as described below and generally dictated a high jet exit velocity. Since it was also important to record the flame at high framing rates, to produce a movie sequence, it was imperative to use a bright flame (thus excluding hydrogen) to ensure adequate light levels. The desire to avoid flame stabilization devices at the burner lip (thus complicating the initial conditions) dictated a fuel with as high a laminar flame speed as possible. These requirements led to acetylene as the fuel of choice. Among the common fuels, it is second only to hydrogen in laminar flame speed [16] and is consequently very resistant to flame blowout. An important additional benefit from using acetylene is the fact that the flame is extremely bright at high flow rates, and produces only a small amount of unburned soot at the flame tip [4, 29]. Our earlier attempts using hydrogen stabilized methane lacked sufficient visible light at the high exit speeds required for this study. Consequently, other common fuels were not tried.

The flow conditions were as follows: exit velocity, U_0 = 230 m/s; exit Mach number, M_0 = 0.7; exit diameter, d_0 = 3 mm; cold Reynolds number Re = $\rho_0 U_0 d_0/\nu_0$ = 76,000; Froude number, Fr = $U_0^2/gd_0 = 1.8 \times 10^6$. In order to estimate the importance of buoyancy, one can model the entire flame as a cone of hot gas of density ρ surrounded by air of density ρ_∞ over a downstream distance x. Hence the ratio of the buoyancy force to the incoming momentum flux is given by

$$\frac{\text{buoyancy}}{\text{inertia}} = \frac{(\rho_\infty - \rho) g \pi/4 d^2 x/3}{\rho_0 U_0^2 \pi/4 d_0^2} < \text{const},$$

which for the worst case of $(\rho_\infty - \rho) \to \rho_\infty$ leads to

$$\frac{\rho_\infty}{\rho_0} \frac{g d_0}{U_0^2} \left(\frac{x}{d_0}\right)^3 < \text{const}, \tag{1}$$

using the fact that the local diameter d is linear in downstream distance x. In order to determine the value of the constant we note that Becker and Yamazaki [1] suggest that for a flame to be momentum driven $\epsilon_L = (\pi g \rho_\infty/4G_0)^{1/3} L$ should be about 2, where G_0 = jet momentum flux and L = flame length. This latter expression is simply the cube root of Eq. 1 for the case of a top-hat exit velocity profile. For $L = 255 d_0$, ϵ_L = 2.2, suggesting that our flow is generally momentum driven (the magnitude of the exit speed illustrates the central difficulty with operating in the momentum driven regime). In this estimate, the flame length was taken to be $255 d_0$, as this was measured from examination of the data. The flame length could also be estimated from the correlation of Becker and Liang [3] or Broadwell [20]. The latter would predict a flame length of $155 d_0$ for acetylene, but, as shown by the extensive data compilation of Dahm and Dimotakis (discussed above), agreement within a factor of 2 is common for

many fuels. In any event, the conditions described here exceed that of most common laboratory flames in both Reynolds and Froude numbers, and generally meet the criteria of Becker and Yamazaki [1] that the flow can be taken to be momentum driven. Thus we expect buoyancy to play only a very minor role in the results to be discussed here.

EXPERIMENTAL DETAILS

Commercial grade acetylene was used in this study. Two cylinders were generally needed to supply the desired flow rate. The burner was designed to produce a uniform, top-hat exit velocity profile with an exit diameter was 3.0 mm. The exit of the burner was located 50 cm from the floor and was centrally located within a 2-m × 2-m × 2.7-m-high double-screened enclosure. An overhead exhaust fan removed all products of combustion. The top of the hood was sufficiently removed so as not to affect the flame. The entire arrangement was located within a large room 3.5 m × 8.8 m in area with the center of the screened enclosure placed along the centerline of the room and 1.8 m from the back wall. The doors of the room were vented as well as portions of the ceiling in order not to starve the overhead fan.

It was observed that the double-screened system (two layers of 15-mesh aluminum screen spaced 1.5 in apart) was very effective in removing unwanted draughts, as evidenced by the fact that, with the overhead fan in operation, the acetylene flow rate could be reduced to very low values to produce a very stable laminar diffusion flame, free from jitter and crossflow. The aluminum mesh screen was painted black to eliminate stray reflections and all photographs discussed below were taken directly through the screens.

All of the movie sequences were made by use of a Kodak Spin Physics SP2000 motion analysis system using a 28 mm f2.8 lens. The CCD camera consists of 192 by 238 pixels of resolution. The camera was located 5 m from the flame. Generally, the flame was framed at 2000 Hz, but data are shown below by skipping every other frame for a net rate of 1000 Hz. The Spin Physics system includes a movable cursor that was used to extract quantitative information from the flame images.

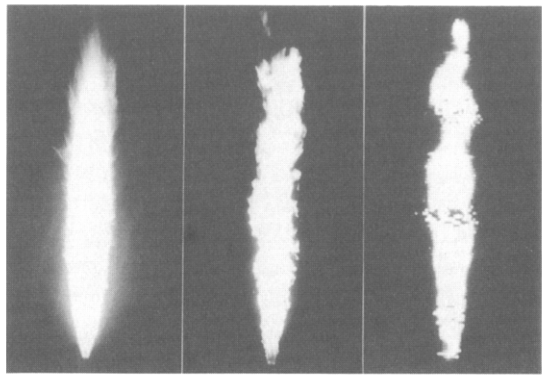

Fig. 2. Realizations of the acetylene flame (a) Time-averaged (1/15 s, 35 mm camera), (b) instantaneous (1/1000 s, 35 mm camera), and (c) instantaneous (1/2000 s, Spin Physics system).

For our conditions the pixel-to-pixel resolution corresponded to 3 mm of the flame.

Because the camera does not have as wide a dynamic range as film, it was convenient to view the output signal from the camera directly on an oscilloscope in order to minimize saturation of the CCD array. This same technique was also used for focusing the camera on the flame. A particularly difficult problem was the fact that the lower half of the acetylene flame is especially bright compared to the upper half, leading to "blooming" of the image (so bright in fact that one would suffer from persistence of vision for several minutes if it were viewed directly). Stopping the camera down to avoid saturation caused significant flame shortening and loss of information. The solution adopted was to use a set of optical neutral density filters strategically placed so as to block the high-intensity, lower portions of the flame while not affecting the upper, low-intensity regions. The camera was then operated with the lens fully open. In this way the flame appearance on the CCD camera is essentially the same as would be captured on film, as is shown in Fig. 2. Flame lengths measured by the CCD camera and by the naked eye were also in good agreement, ensuring no artificial shortening.

RESULTS AND DISCUSSION

Figure 2 shows the flame as recorded by use of photographic film (Kodak Tri-X, 400 ASA) at

1/15 s time exposure and 1/1000 s exposure, and a similar photo shot directly from the Spin Physics video monitor. The video image is 1/2000 s exposure and is statistically independent of the other images. All images have been printed to the same size to maximize detail. The first of these is similar to other time-exposed images of turbulent diffusion flames (see Ref. 4) and can be used to visually estimate a flame length. In this case, the visible flame length from burner lip to flame tip is about 75 cm, or $250d_0$. The second photo shows the instantaneous burning and is of course significantly different from the time-averaged view. The third photo from the Spin Physics video monitor is shown to compare the quality of its image with that obtained from film. Although clearly not as good, the image contains sufficient detail for our purposes, as is discussed later (this image, and subsequent images also contain some rows of bad pixels that should be ignored). It is useful to note at this point that the instantaneous images look turbulent, but organized structure is not immediately apparent. We shall return to this issue when the movie sequences are discussed later.

Becker and Yamazaki [1] have discussed in some detail the difficulty of defining the flame length. This could take many forms, such as visual observation by several observers, use of time-exposed photographs such as Fig. 2a, averaging of several photos such as Figs. 2b and 2c, or use of the mean temperature profile to ascertain the point at which maximum mean centerline temperature is achieved before dilution of the combustion products occur. Each of these techniques can lead to different measures of the flame length in terms of number of initial jet diameters. These differences, however, are generally not large. For the purposes of this work the flame length is defined by averaging the visible light as recorded for 2000 photographs such as Fig. 2c. Because we are primarily interested in flame tip dynamics, the exact definition used is not a crucial issue.

Figures 3a and 3b show a continuous sequence of photos 1/2000 s exposure, each 1/1000 s apart, of the development of the burning turbulent jet photographed directly from the video monitor. Since no flame stabilization is used, the flame base is lifted by about $10d_0$ but appears more so because the filtering technique was maximum at the base and the initial blue stabilization region is not captured by the Spin Physics camera. In these photos, the exit nozzle is located at the base of each frame, with the horizontal line on the first image set at the 80 cm downstream location. Each one of these photos appears turbulent and more random than when organized on a frame by frame basis, so that any large-scale organized structure is not obvious at first glance. These photos are equivalent to the movie sequence of a liquid flame of Dahm and Dimotakis shown in Fig. 1a. The differences are now that this is a burning gaseous jet, all of the emitted light is captured rather than a slice along the centerline plane, and a much longer record is shown to provide a sense of the flame evolution with time. In any event, the repetitive burnout of the flame tip is especially noteworthy. The reader is encouraged to sight along the time axis to more easily see the evolution of the flame tip.

These photos suggest that the flame tip often consists of an organized structure that convects downstream and is entraining air from its upstream side, as evidenced by the fact that the fuel first burns out at the upstream edges and appears to separate from the main body of the jet. This is not a fluid mechanical separation, but merely the fact that the entrained air has consumed the available fuel at that location. The structure eventually burns out as it convects downstream. At this point the visible flame drops back to the next available upstream (fuel-bearing) structure, which then continues downstream, entrains air, and burns out by essentially the same mechanism. It is also clear that at times a substantial fraction of the overall flame (as much as 40%) can be involved in this burnout process. Fig. 3 also shows the critical importance of the use of a movie sequence rather than still photos. Single uncorrelated frames simply do not demonstrate large-scale organization. It requires high-framing-rate photography and the chemistry of the burning process for structure to reveal itself.

It is now possible to determine the organized structure in Fig. 2c. This photo is the first photo of Fig. 3a—the movie sequence now reveals the future development of the tip. It is also useful to

attempt to track, backwards in time, the development of a particular structure that eventually becomes the flame tip. Sometimes the beginnings of organized burnout are discernible as far back as the midpoint of the overall flame length, which then proceeds down to the flame tip. This is evidence of the fact that the tip burnout is the culmination of an organized motion that often begins to be discernible long before actual tip burnout occurs. When compared with the liquid flame results, we must conclude that this is part of the momentum driven entrainment process and not a consequence of buoyancy. Dibble et al. [30] once seeded a hydrogen jet flame with Freon-12 and produced photos of what appears to be tip oscillation. However, the framing rate was insufficient to record the evolution of the structures from one frame to the next.

We think it interesting that the tip oscillation phenomenon under momentum driven conditions has not been investigated in the past. The reasons have probably to do with the fact that large-scale organized motion is only just beginning to be recognized in the far field of nonreacting jet flows, with the combustion implications yet to be fully documented. In fact the motivation to look for this phenomenon came only after seeing the liquid flame sequences. A further difficulty is the fact that momentum-driven jet diffusion flames are generally high-speed affairs, leading to little measurable light signals, flame stability problems and high framing rate. For comparison, the liquid flames were at a Reynolds number of 10,000 and required a framing rate of only 40 Hz. Furthermore in the liquid case, a change in the acid-base chemistry could be used to cause the burnout phenomenon to occur at any desired (far-field) axial station using the scaling arguments of Broadwell [20]. In our case, the stoichiometry of acetylene-air determines this location, and no

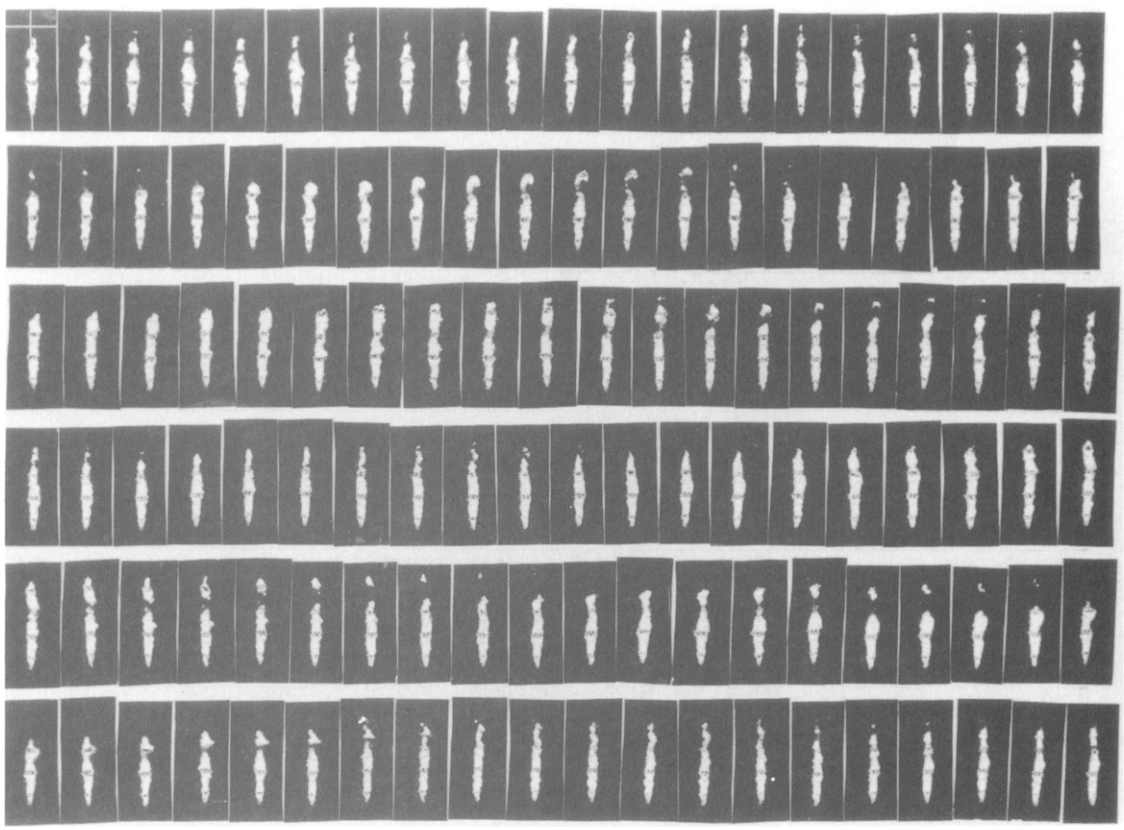

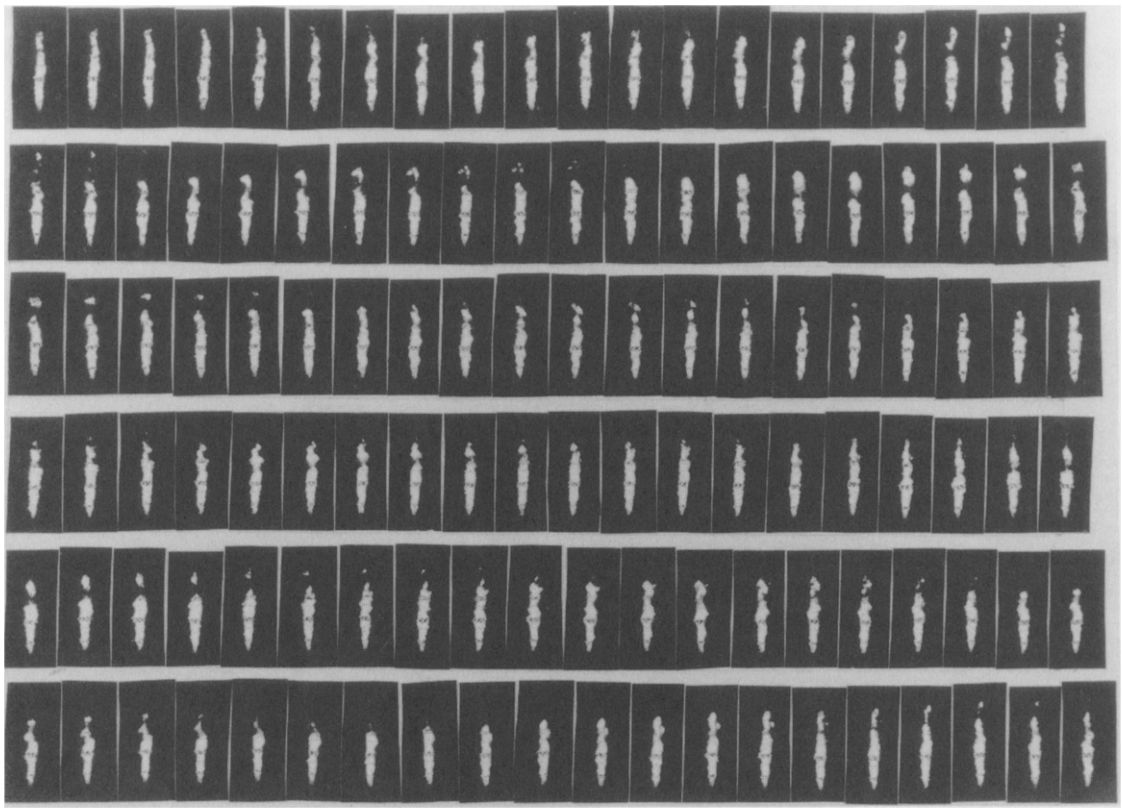

Fig. 3a, b. Continuous movie sequence of burning acetylene flame. Each frame 1/2000 s exposure, spaced 1/1000 s apart. Time increases from left to right, then top to bottom. Jet exit at base of each frame, horizontal line on first frame at 80 cm downstream location.

attempts at dilution of the fuel stream were used to change the tip location. Thus although the flame tip burnout has been demonstrated here at about 250 initial diameters downsteam, we believe the same phenomenon to be occurring in the concentration field in a self-similar way throughout the jet as we proceed downstream. The flame tip is simply the unique location where one can see final burnout without the complications of the neighboring downstream structure obstructing the view. Also as discussed above we do not consider this to be a buoyancy-driven phenomenon but a fundamental feature of momentum-driven jets.

It is also quite interesting that when the camera aperture is significantly stopped down, the flame can be made to shorten considerably (due to lack of light), but that the same phenomenon of tip burnout continues to be observed, at a closer axial location, and of course at a higher frequency. It is also useful to reiterate that a shadowgraph image of the flow simply shows a 25 degree spreading angle, with no particular evidence of the organized motion that is being discussed here since the three-dimensional nature of the organized structure is obliterated by the shadow method.

Figure 4a shows the instantaneous flame length variation as a function of time for 250 frames (0.25 s duration). Here the flame length is simply the last visible point before the soot emission disappears. This plot merely shows the quasiperiodic nature of the flame burnout with the attendant rapid dropback to the next combustible structure. Once again such a time trace looks "turbulent," however it must be noted that the data points are heavily clustered on the rising portion of the time trace, and very few data points

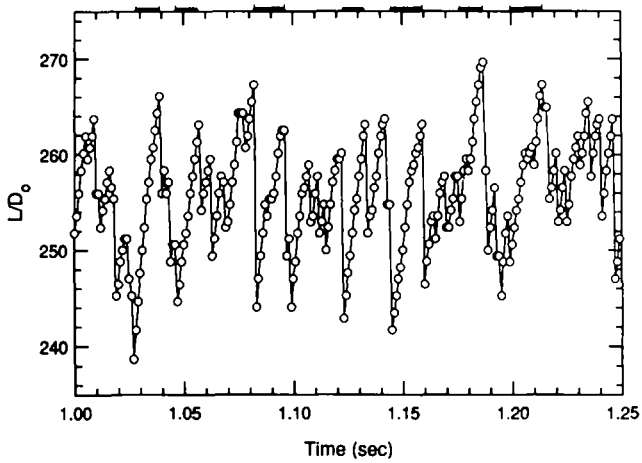

Fig. 4a. Plot of instant flame length as a function of time to show flame tip burnout. Tick marks indicate events for which tip burnout was counted.

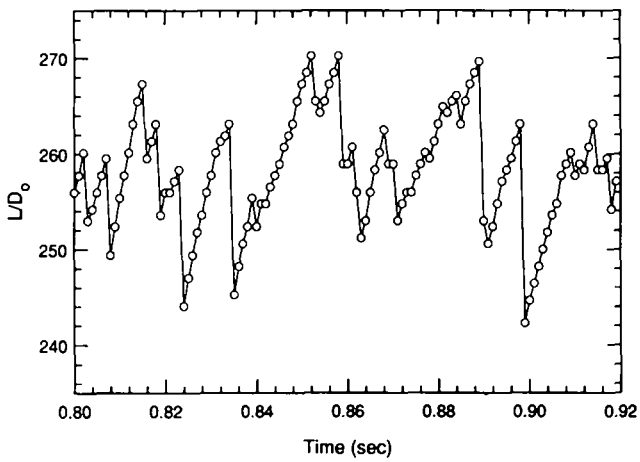

Fig. 4b. Plot of instantaneous flame length corresponding to Fig. 3a.

on the dropback portion. Figure 4b similarly shows the instantaneous flame length as a function of time for 120 frames (0.12 s duration) corresponding to the sequence shown in Fig. 3a so that the reader is able to compare both. In general, the photos, Fig. 3, containing much more information, are better able to show the physical extent of the region over which burnout is about to occur, whereas the flame length measurements simply select the maximum available light. It is also clear that there are times when the tip itself shows little motion, but the portions of the flame upstream of it start to show the beginnings of organization. Good examples of this are shown in fourth row of Fig. 3a and the fourth row of Fig. 3b.

Figure 5 shows a histogram of the measured instantaneous flame lengths for 2000 frames (2 s duration). This suggests a mean value of $255d_0$, which is in good agreement with Magnussen [5] and the predictions of Becker and Liang [3]. In any event, as was remarked earlier, various techniques for defining the flame length lead to somewhat different estimates. A plot such as this, in effect, washes out the growth and dropback evolution discussed above. The gaussian shape might suggest the tip to be a random variable in the statistical sense, but the movie sequences and time traces discussed above certainly suggest otherwise. This is one example of a modest amount of averaging seriously masking the mechanistic features of the flame.

Figure 6 shows the distribution of burnout

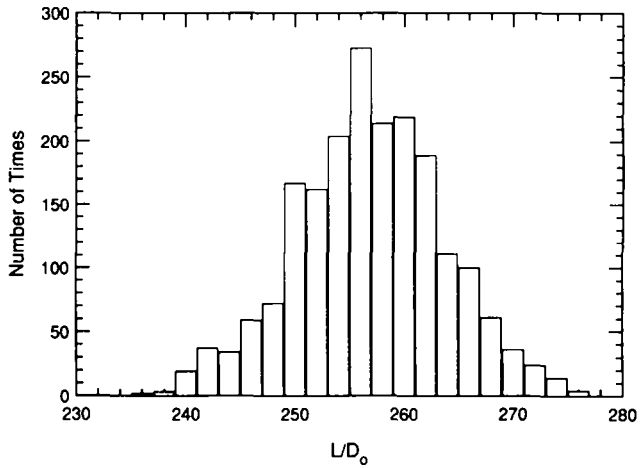

Fig. 5. Histogram of flame length measurements using 2000 (2 s) realizations.

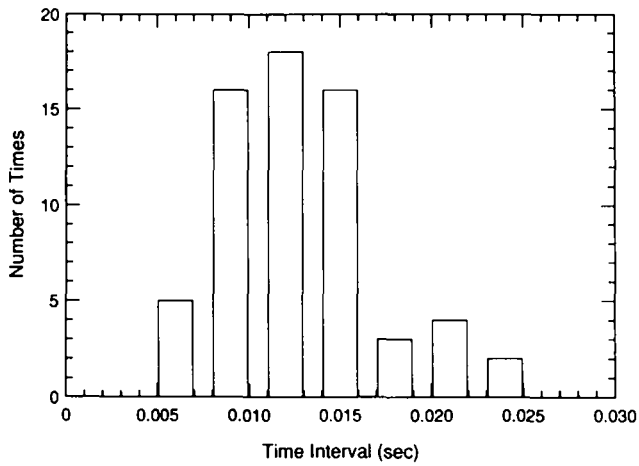

Fig. 6. Histogram of time intervals of flame length fluctuations.

times. This was defined as the time intervals from one dropback to the next and were established from plots such as Fig. 4a. In preparing such a plot, it was necessary to choose events for which a clear, unambiguous burnout occurs. This occurs about 50% of the time with sample events shown on Fig. 4a. Smaller oscillations of the flame tip for which the burnout and dropback are less clear were not counted (we shall return to this issue later). In order to estimate the large-scale time, the results of Becker and Yamazaki [1] for a momentum-driven flame are used to estimate the centerline velocity, while the growth rate is taken from the fact that the jet half-width is about $0.2x$. For a momentum-driven flame, Becker and Yamazaki show that

$$\frac{U_c}{U_0} = 6.2 \left(\frac{\rho_0}{\rho_c}\right)^{1/2} \left(\frac{x}{d_0}\right)^{-1},$$

where ρ_c is the mean centerline density. Because the adiabatic flame temperature is 2600 K for acetylene-air, at the flame tip we would expect about 70%–80% of this value as a mean value. Using 75% as a representative value yields $U_c \sim$ 15 m/s at $255d_0$, with the large scale time given as 0.011 s, which should be compared with the values shown in Fig. 6. Thus the conclusion to be drawn from this plot is that when the structure is clearly visibly organized in an axisymmetric fash-

ion, the characteristic time is comparable to that of the large-scale structure.

An interesting question is what happens during the other 50% of the time when a clear characteristic burnout is not observed. Closer inspection of Fig. 3 suggests two types of behavior—in the first, the entrainment and burnout appear axisymmetric, the flame appears as discussed by Dahm and Dimotakis, with entrainment from the backside and a somewhat rounded tip. In what appears a second mode, the flame has a more pointed appearance at the tip, is generally long and sinuous and usually does not show obvious backside entrainment. The tip appears to burn out more by "dissolving" away in the radial direction (good examples of this are seen in the fourth row of Fig. 3a and the first row of Fig. 3b). We can only speculate that at these times the jet may be in a possible spiral mode, different from the axisymmetric mode and with a correspondingly different entrainment pattern. Becker and Liang [7] discuss various axisymmetric and sinuous instabilities for a low-Reynolds-number acetylene flame, but it is unclear if these would be apparent at the Reynolds numbers of this work. There also exist a large body of data on the various instability modes of nonreacting jets that suggest the existence of axisymmetric as well as helical modes (see for example Refs. 31–33). In the absence of buoyancy, it seems reasonable that these modes continue to exist for the reacting jet.

Consideration of the instability modes has some appeal, and leads to the following speculative rationalization of the observed turbulent combustion process: (1) given the flow, there exist dominant, unstable modes, (2) associated with the vorticity field of each mode is a unique entrainment pattern, and (3) each entrainment pattern must then result in a characteristic appearance of the flame as fuel and oxidizer mix and burn. By this approach, a two-dimensional mixing layer would be primarily Kelvin-Helhholtz unstable, leading to the well known two-dimensional rollers [19, 34]. For a jet the situation is more complex, as axisymmetric, helical, and double helical modes are possible. However, the entrainment pattern of each mode should be unique and with observable combustion implications. The suggestion from our data here is that the jet was in the axisymmetric mode about 50% of the time. The remaining time corresponds to situations where the tip showed no clear axisymmetric burnout but was often in transition from, or evolving to, the next axisymmetric event (Fig. 3). Consideration of axisymmetric (Fig. 1b) and helical entrainment patterns (Fig. 7), would suggest different flame appearances associated with each instability mode. The Dahm and Dimotakis picture of a separating flame tip would probably be valid for the axisymmetric case because of the resultant backside entrainment (Fig. 1b). A possible nonseparating, sinuous tip that dissolves away due to more radial entrainment could result from the helical case (Fig. 7). The speculative ideas presented here are generally consistent with those presented in Refs. 35 and 36 concerning the implications of organized structure upon mixing and combustion.

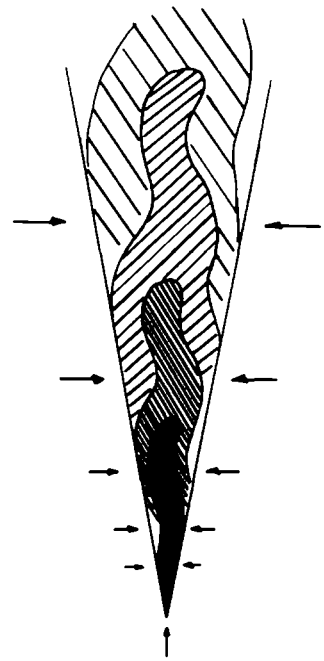

Fig. 7. Expected concentration field and entrainment pattern for the helical mode of a round turbulent jet (to be compared with the axisymmetric mode of Fig. 1b).

It is also clear that a discrepancy exists between the liquid flame and the gaseous flame reported here. One might ask why the liquid flame appears to be more in the axisymmetric mode than the

gaseous flame. Part of the difference may have to do with the facilities used: for the liquid experiments, the water tank used has an inherent axisymmetric flow recirculation pattern, whereas for the burning jet, exhaust product is removed from the overhead hood. It is conceivable that slight amounts of swirl in the entrained air could be enhanced in this configuration, more so than the liquid experiments, leading to different appearances.

Magnussen [4, 5] has reported soot measurements taken along the centerline of a 3 mm diameter, $U_0 = 176$ m/s acetylene jet at $x/d_0 = 120$. This would correspond to a location that is just under half of the visible flame length. He indicates significant intermittency associated with the time traces of soot concentration and the fact that it scales with the large scale time. We believe that Fig. 3, the flame tip oscillation discussed here (indicative of large structure organization) and the soot measurements of Magnussen are consistent. The argument proceeds as follows; at the flame base region the acetylene soots heavily and any soot precursors (see Ref. 37) and unburned soot are transported by the large-scale motion throughout the jet. This process continues as one proceeds downstream and we would consequently expect soot to occur more or less uniformly throughout the large-scale structure, because of the high Schmidt number of the soot particles (Magnussen presented only single point measurements, so the expected uniformity and radial correlation of soot cannot be checked). This process continues as one proceeds downstream with the fuel being diluted with product and soot particles. Towards the flame tip region, the situation is such that the fuel is now the minority species and the entrained air causes the fuel to be consumed as shown in Fig. 3. Soot that cools radiatively below 1300 K [8, 29] is not consumed and escapes past the flame tip as unburned carbon. The crucial feature of this discussion is that an organized motion exists in momentum-driven jet flows and that its consequences can be manifested in measurements such as those of Magnussen and the ones reported here. Gore and Faeth [9] have recently swept a laser beam through an acetylene flame 80–90 diameters downstream and observed that the soot is confined to streaks, "probably associated with the eddy structure of the flame, similar to the earlier observations of Magnussen."

Finally, we note that other examples of large-scale, far-field organization are now being reported. Recently, Schefer and Dibble [38] used single-point Rayleigh scattering to infer mixing at various axial stations in a round turbulent jet. Power spectra of the scalar field taken at 15 diameters downstream show no preferred frequencies, whereas at 30 diameters a 630 Hz dominant frequency is found and at 50 diameters a dominant frequency of 250 Hz is measured. Although the authors do not note it, these two frequencies at 30 and 50 diameters scale appropriately with the large-scale growth (linear in x) and velocity decay (inverse with x) so that given the 630 Hz value at 30 diameters, one would predict a value of $630 \times (3/5)^2 = 277$ Hz, which is quite close to the measured 250 Hz (the jet is ducted so one would expect the free jet scaling to underpredict the large-scale frequency). The fact that no dominant frequency is seen at 15 diameters is consistent with the fact that the jet is evolving from near-field to far-field behavior, and that the organization is not a remnant of some near-field instability, as would be the case for a highly buoyant jet [2]. Additional important work by Dowling [39], has recently shown directly that the probability density function (pdf) of mixture fraction is self-similar past 20 jet diameters downstream. Hence self-similarity of the scalar field is equivalent to saying that phenomena such as flame tip oscillation measured at any far-field location is representative of the entire far-field.

CONCLUSIONS

These experiments have sought to examine the flame tip dynamics of a momentum driven turbulent jet flame. This results show that the flame tip burnout is quasi-periodic in nature, an event that is governed by the large-scale motion of this flow. Single uncorrelated photos do not reveal the organized structure and a high framing rate movie sequence is required to observe this phenomenon. The movie sequences suggest two types of behavior—axisymmetric, in which the visible flame tip

is rounded in appearance and detaches from the main flame body, and possibly helical, in which the tip is more pointed in appearance and fails to detach from the main flame body. It is suggested that consideration of the instability modes of the jet, and the resulting entrainment patterns provides a reasonable approach to understanding the observed flame structure.

The results are similar to the liquid flame results of Dahm and Dimotakis, which show that flame tip burnout is a consequence of organized motion. The picture proposed here is one in which entrained air enters the jet. Close to the jet exit the air is the lean reactant, and the products, soot, and soot precursors that are formed mix with and dilute the fuel stream with downstream distance. This process continues until at the flame tip the remaining fuel is the lean reactant that the entrained air finally consumes throughout the jet. For the axisymmetric mode, this entrainment probably occurs primarily from the upstream side and explains the flame detachment at the tip. Once the burnout is complete the flame becomes visible (drops back) to the next incoming structure, which burns out in similar fashion. For the helical mode the entrainment is probably more radial such that the flame does not detach from the main flame body and shows a more pointed flame tip appearance. Judging by its appearance, the flame also appears to continuously evolve from one mode to another over time.

These observations may also help to explain the soot measurement of Magnussen, namely that significant amounts of soot occur in eddies that are related to the organized structure. It should be noted that these results are not due to buoyancy because of the high Froude numbers employed in this work. Studies at lower Froude numbers would suggest the flow to be more dominated by the axisymmetric mode, and are currently in progress.

We wish to thank J. E. Broadwell for many useful discussions about turbulent mixing in round jets, W. J. A. Dahm for discussion about the liquid flames, and C. T. Bowman for use of the Spin Physics recording system.

REFERENCES

1. Becker, H. A., and Yamazaki, S., *Combust. Flame* 33: 123-149 (1978).
2. Miake-Lye, R. C., and Toner, S. J., *Combust. Flame* 67: 9-26 (1987).
3. Becker, H. A., and Liang, D., *Combust. Flame* 32: 115-137 (1978).
4. Magnussen, B. F., *Fifteen Symposium (International) on Combustion,* The Combustion Institute, 1975, pp. 1415-1425.
5. Magnussen, B. F., Hjertager, B. H., Olsen, J. G., and Bhaduri, D., Seventeenth Symposium *(International) on Combustion,* The Combustion Institute (1978), pp. 1383-1393.
6. Becker, H. A., and Liang, D., *Combust. Flame* 44: 305-318, (1982).
7. Becker, H. A., and Liang, D., *Combust. Flame* 52: 247-256 (1983).
8. Kent, J. H., and Bastin, S. J., *Combust. Flame* 56: 29-42 (1984).
9. Gore, J. P., and Faeth, G. M., Structure and properties of luminous turbulent acetylene/air diffusion flames. AIAA-87-9298, 1987.
10. Becker, H. A., and Yamazaki, S., *Sixteenth Symposium (International) on Combustion,* The Combustion Institute, 1976, pp. 681-691.
11. Becker, H. A., Liang, D., and Downey, C. I., *Eighteenth Symposium (International) on Combustion,* The Combustion Institute, 1981, pp. 1061-1071.
12. Chen, L.-D., and Roquemore, W. M., *Combust. Flame* 66: 81-86 (1986).
13. Strawa, A. W., and Cantwell, B. J., *Phys. Fluids* 28: 2317-2320 (1985).
14. Chigier, N. A., and Yule, A. J., The Project SQUID Technical Report US-1-PU (1979).
15. Kalghatgi, G. T., *Combust. Sci. Technol.* 41: 17-29 (1984).
16. Kalghatgi, G. T., *Combust. Sci. Technol.* 26: 233-239 (1981).
17. Hottel, H. C., *Fourth Symposium (International) Combustion,* The Combustion Institute, pp. 97-133.
18. Dahm, W. J. A., and Dimotakis, P. E., *AIAA J.* 25: 1216-1223 (1987).
19. Brown, G. L., and Roshko, A., *J. Fluid Mech.* 64: 775-816, (1974).
20. Broadwell, J. E., A model of turbulent diffusion flames and nitric oxide production. TRW Doc. 38515-6001-UT-00, Redondo Beach, CA 1982.
21. Tyson, T. J., Kau, C. J., and Broadwell, J. E., A model of turbulent diffusion flames and nitric oxide generation—part II. Energy and Environmental Research Corporation Report, 1982.
22. Bilger, R. W., and Beck, R. E., *Fifteenth Symposium (International) on Combustion,* The Combustion Institute, 1974, pp. 541-522.

23. Peters, N., and Donnerhack, S., *Eighteenth Symposium (International) on Combustion,* The Combustion Institute, 1981, pp. 33–42.
24. Broadwell, J. E., Dahm, W. J. A., and Mungal, M. G., *Twentieth Symposium (International) on Combustion,* The Combustion Institute, 1984, pp. 303-310.
25. Dahm, W. J. A., and Dibble, R. W., *Twenty-second Symposium (International) on Combustion,* The Combustion Institute, 1988, pp. 801-808.
26. Bilger, R. W., *Twenty-second Symposium (International) on Combustion,* The Combustion Institute, 1988, pp. 475-488.
27. Peters, N., and Williams, F. A., *AIAA J.* 21: 423–429 (1983).
28. Williams, F. A., *Combustion Theory,* 2nd. ed., Benjamin/Cummings, Menlo Park, CA, 1985.
29. Kent, J. H., *Combust. Flame* 67: 223-233 (1987).
30. Dibble, R. W., and Schefer, R. W., Chen, J. Y., Hartmann, V., and Kollman, W., SANDIA Report SAND85-8233, 1987.
31. Batchelor, G. K., and Gill, A. E., *J. Fluid Mech.* 14: 529-551 (1962).
32. Browand, F. K., and Laufer J., in *Fourth Symposium on Turbulence in Liquids.* University of Missouri-Rolla (J. L. Zankin and G. K. Patterson, Eds), Science, Princeton, NJ 1977.
33. Tso, J., and Hussain, A. K. M. F., *J. Fluid Mech.* 203: 425–448, (1989).
34. Mungal, M. G., and Dimotakis, P. E., *J. Fluid Mech.* 148: 349–382 (1984).
35. Broadwell, J. E., and Dimotakis, P. E., *AIAA J.* 24: 885–889 (1986).
36. Dimotakis, P. E., and Miake-Lye, R. C., and Papantoniou, D. A., *Phys. Fluids* 26: 3185–3192 (1983).
37. Haynes, B. S., and Wagner, H. G., *Prog. Ener. Combust. Sci.* 7: 229-273 (1981).
38. Schefer, R. W., and Dibble, R. W., Rayleigh scattering measurements of mixture fraction in a turbulent nonreacting propane jet. AIAA-86-0278, 1986.
39. Dowling, D. R., Mixing in gas phase turbulent jets, Ph.D. thesis, Caltech, 1988.

Received 5 January 1988; revised 18 November 1988